*J. Phys. Chem. A* **2000,** *104,* 2341−2350

# Configuration Interaction between Covalent and Ionic States in the Quantal and Semiclassical Limits with Application to Coherent and Hopping Charge Migration

**F. Remacle**[†]
*Département de Chimie, B6, Université de Liège, B 4000 Liège, Belgium*

**R. D. Levine***
*The Fritz Haber Research Center for Molecular Dynamics, The Hebrew University, Jerusalem 91904, Israel, and Department of Chemistry and Biochemistry, University of California—Los Angeles, Los Angeles, California 90095*

*Received: August 19, 1999; In Final Form: November 11, 1999*

Charge transport in molecular and extended systems is discussed with special reference to the mixing of covalent and ionic states and the evolution of this mixing with time. The formalism allows the electron to acquire an extra phase when it moves from one site to the next so that a hopping limit can be reached where the electron transfers with a random phase. The equations of motion are solved for both quantum mechanical and classical dynamics. An appendix discusses a classical representation of orbital occupancies in a manner consistent with the Pauli exclusion principle.

## 1. Introduction

The molecular orbital (MO) approach to the electronic structure of molecules and of extended structures[1,2] is a well developed tool, equally useful for spectroscopy and for understanding the geometrical structure and other properties of the ground state. But already 50 years ago Coulson and Fischer[3] pointed out that the MO wave function gives equal weight to covalent and ionic structures. As the bond distance is increased, the weights are not allowed to change, and so, asymptotically, $H_2$, for example, dissociates equally to H + H and $H^+ + H^-$. In reality, the ionic channel has a much higher threshold, being the difference between the ionization potential (IP) of the H atom and its electron affinity. Coulson and Fischer[3] introduced a more flexible wave function which can be regarded as a linear combination of the molecular orbital and the primitive valence bond (VB) wave function of Heitler and London. The latter assigns each electron to an atom and so dissociates uniquely to H + H. More recently, Goddard[4−6] showed how to achieve the same aim by retaining the form of the valence bond wave function without however restricting the “atomic” wave functions to being necessarily strictly localized.

The same limitation on the MO wave function arises when one wants to discuss charge transfer or charge migration in molecules. In particular, the simple tight binding model of electrical conductivity suffers from the defect that there is no energy penalty when two electrons (of opposite spins) occupy the same site. In solid-state physics, the required modification of the tight binding Hamiltonian so as to incorporate this, so-called, “Coulomb blocking” is usually attributed to Hubbard.[7] Theoretical chemists, on their own, have seen the same need, and the Hamiltonian that incorporates this effect is familiar as that of Pariser−Parr−Pople (PPP).[8−10] The PPP Hamiltonian includes not only the electrostatic repulsion of two electrons on the same site but also when the two electrons are on different sites.

There is a methodological difference between the routes discussed in the two paragraphs above. In the second paragraph, one does not attempt to diagonalize the full Hamiltonian. Rather, one tries to construct a model Hamiltonian, which has much of the physics built in. Then one solves for this Hamiltonian. For reasons that are obvious, what one often does is to force an orbital description on the wave function. For either the Hubbard or the PPP Hamiltonians, a single determinant wave function cannot be exact because the Hamiltonian explicitly has terms that impose correlations between different electrons. So one usually solves the problem using a self-consistent field (SCF) procedure.

In this paper, we use the PPP Hamiltonian, but diagonalize it exactly by making a complete configuration interaction (CI). That, of course, is not the same as a complete unrestricted configuration interaction because the PPP Hamiltonian is only an approximation. It fails to allow for three and four site terms. But for the problems that we want to address, the full CI goes well beyond an SCF solution. The technical foundations for doing the complete configuration interaction have been provided by Paldus,[10] Matsen,[11] Shavitt,[12] Pauncz,[13] and many others (see ref 14). We will particularly use the basis set pioneered by Paldus.[10]

We introduce a minor extension to the PPP Hamiltonian, which will allow us to discuss electron transport in a more realistic (but phenomenological) fashion. In its familiar form, the PPP Hamiltonian contains one and two center electronic integrals. In reality, there are additional (three and four center) interactions and these are neglected. What is the physical effect of the neglected terms? Take as an example the one-electron “transfer” integral, denoted $\beta$ in simple MO theory. This transports an electron from an atom to its near neighbor. This transfer is coherent, and in an extended array it can lead to a conduction band where the electron can move coherently

---

* Corresponding author. Fax: 972-2-6513742; E-mail: rafi@fh.huji.ac.il.
[†] Chercheur Qualifié, FNRS, Belgium.

10.1021/jp992924i CCC: $19.00

throughout the lattice. The wave function is a Bloch wave in solid-state physics[15,16] or a delocalized MO in molecular physics. But physically the transferred electron interacts with other electrons, particularly those on the same site. We will see (cf. Figure 2 and ref 17) how including the two-electron Hubbard term causes a dephasing of the migrating charge. In the present work, the two-electron interaction is explicitly allowed, but there are also three or four site terms which are not in the Hamiltonian that we use. As a result of these extra terms, the transferred electron is scattered, and due to the Pauli restrictions, the scattering is primarily elastic. So the transferred electron acquires an additional phase. We allow for this effect by making $\beta$ complex but Hermitian. Specifically, we write the transfer integral between neighboring sites $i$ and $j$ as

$$\beta ij \to |\beta|\frac{1}{2}\,(1+\exp(2i\delta_{ij})),\quad \beta ji = \beta ij^{*}$$

The magnitude of the additional phase shift $\delta ij$ determines the loss of coherence per an elementary transfer. The limit of incoherent transport is when the phase shift $\delta$ is so large that, modulo $2\pi$, it is random. Note, however, that even with this modification we remain within a Hamiltonian formalism so that energy relaxation effects[18] are not included.

The other problem we address is that, for complete configuration interaction, the scaling of the computational effort with the number of atoms is prohibitive. As an example, we are interested in two-dimensional hexagonal arrays of "artificial" or "designer" atoms.[19,20] Each such atom is a cluster or a "nanodot" which we approximate as an atom with one valence electron. The physical point is that due to their large size; these designer atoms have an unusually low value of the Coulombic repulsion between two electrons on the same site. This brings the energy of the excited ionic states lower than is the typical case for molecules. It is therefore not possible to approximately treat these states, and so a proper configuration mixing is called for. There are 784 (doublet) basis states for a seven-electron, seven-site problem. This sized Hamiltonian matrix can be readily handled. For the next completed hexagonal lattice, with two layers around the central atom, there are 19 sites. For 19 electrons on this 19-site lattice, eq 3.2 indicates that there will be 2 821 056 160 doublet basis states. Yet our experimental colleagues (correctly) feel that even 19 sites is a very small hexagonal array. So we need some drastic reduction in computational effort. We need a method that scales linearly with the number of electrons. In classical mechanics, that is what will be the case. Each particle in the problem increases the effort by adding two first-order differential equations of motion (position and momentum). We will, of course, work with action-angle variables,[21,22] but the need to impose the limitations of the Pauli principle means that the transition from a quantal to a classical Hamiltonian, implemented in section 4, is not quite trivial. Essential background technical details for this limit are provided in Appendix B.

In the interest of brevity, we do not elaborate the details of the physical problems for which the formalism is useful. Specifically, there are two, and quite distinct, systems which we have considered. One is the already alluded to optical and electrical response of arrays.[19,20] The other is charge migration and dissociation of molecular cations.[17,23−25] In brief, the chain cation is modeled as a linear molecule, made of "atomic" sites. The rightmost site is chromophoric and is the site where ionization occurs. The bond-breaking energy is lower when the charge is at either side of the bond. So reactivity follows the migration of the charge. The experimental observation[25,26] is that dissociation often does not occur at the site of the initial ionization but rather at the other end of the molecule. In other words, charge migration can (but not necessarily) occur prior to dissociation. We have discussed the competition between (coherent) charge migration and dissociation. In this manuscript, we focus on not completely coherent charge migration. Charge transfer[27,28] is of course of much theoretical interest in many areas, not the least of which is in molecular electronics.[29]

The paper is organized as follows. Section 2 defines the quantum mechanical Hamiltonian we use, with additional technical details given in appendix A. Quantal computations on charge migration, with a special emphasis on the role of dephasing, are presented in section 3. The classical limit is taken in section 4, and many of the more technical details are discussed in appendix B. A comparison of classical and quantum computations is the subject of section 5.

## 2. The Quantum Mechanical Problem

The system we discuss is a linear array of $n$ sites. In the computations reported below, there is one orbital per site, which can accommodate zero, one, or two (of opposite spin) electrons. We will introduce some effect of the possible role of other electrons on a given site in eq 2.3 below, but this is done in a phenomenological manner.

The form of the many-electron Hamiltonian is

$$H = H_0 + H_1 \tag{2.1}$$

where $H_0$ is a one-electron Hamiltonian of the tight binding (or Hückel) type,[9,30,31]

$$H_0 = \sum_{i,j}^{n} h_{i,j} \sum_{\mu}^{2} a^{\dagger}_{i,\mu} a_{\mathrm{j},\mu}$$
$$h_{i,j} = \begin{cases} a_{\mathrm{i}} \text{ if } i = j \\ \beta_{\mathrm{i,j}} \neq 0 \text{ for near neighbors only} \end{cases} \tag{2.2}$$

and $H_1$ are the electrostatic, two-electron terms, cf. eq 2.4 below. The $a^{\dagger}$ and $a$ in eq 2.2 are the creation and annihilation operators for an electron at a given site and with a given spin ($\mu$ = up or down). The sites need not have equal energies α, and the actual values that are used in the computation are listed in the legend of Figure 1. $\beta$ is the transfer integral. Any internal structure of a site is a source of modulation of $\beta$. In the one electron picture, the migrating electron moves into or out of the site orbital. In reality, the electron is scattered. Even if the scattering is elastic, the electron acquires an extra phase and this phase can be different for different sites. In section 4, we shall argue what scattering theorists will know, that we only really care about the value of the phase modulo $2\pi$. Hence, if the phase is large compared to $2\pi$, the part that matters is effectively random. It follows that the simplest correction for the role of the internal structure is to replace the otherwise real $\beta$ by a complex scattering amplitude. This change is equivalent to the substitution

$$\beta_{\boldsymbol{ij}} \to |\beta|\,\frac{1}{2}(1+\exp(2i\delta_{ij})),\quad \beta_{\boldsymbol{ji}} = \beta\boldsymbol{*}_{\boldsymbol{ij}} \tag{2.3}$$

In order that the matrix $\boldsymbol{\beta}$ remains Hermitian, we impose the additional condition $\beta_{ji} = \beta^{*}_{ij}$ so that the Hamiltonian can be diagonalized by a unitary transformation.

The explicit form of the PPP Hamiltonian is

$$H = \underset{\text{one-electron part}}{\sum_{i,j}^{n} h_{ij} \sum_{\mu}^{2} a^{\dagger}_{i,\mu} a_{j,\mu}} + \underset{\text{on site Coulomb repulsion}}{\frac{1}{2} I \sum_{i} \hat{n}_i(\hat{n}_i - 1)} + \underset{\text{cross site Coulomb repulsion}}{\frac{1}{2} \gamma \sum_{i,j} \hat{n}_i \hat{n}_j} \qquad (2.4)$$

where the first term is the one-electron Hamiltonian, $H_0$, discussed above, eq 2.2. The new operators (indicated by a carat) that enter are the number operators for the different sites

$$\hat{n}_i \equiv \sum_{\mu} a^{\dagger}_{i,\mu}\, a_{i,\mu} \qquad (2.5)$$

which sums over both directions of the spin. A binary product of number operators is a two-electron operator.

To diagonalize this Hamiltonian exactly (which is equivalent to a full configuration interaction (CI)), we rewrite it in terms of the generators, $\hat{E}_{i,j}$,

$$\hat{E}_{i,j} \equiv \sum_{\mu}^{2} a^{\dagger}_{i,\mu} a_{j,\mu}, \quad i,j = 1, ..., n$$
$$\hat{E}_{i,j} = \hat{n}_i \qquad (2.6)$$

of the unitary group $U(n)$ ($n$ is the number of sites).[10,11,14]

$$H = \sum_{i=1}^{n} \alpha_i \hat{E}_{i,i} + \beta \sum_{i,j}^{n}{}' E_{i,j} + \frac{I}{2} \sum_{i=1}^{n} \hat{E}_{i,i}(\hat{E}_{i,i} - 1) + \frac{\gamma}{2} \sum_{i,j}^{n} \hat{E}_{j,j} \hat{E}_{i,i} \qquad (2.7)$$

The prime on the second sum indicates that $i$ and $j$ are near neighbors. Note that only diagonal operators appear in the two-electron terms. As will be discussed, this makes the analytical form of the Hamiltonian matrix quite simple. Specifically, we represent the Hamiltonian in a spin-adapted many-electron basis set that belongs to an irreducible representation of the group $U(n)$ (Gelfand–Tsetlin states).[14] These zero-order states we label as the "site states" because they have sharp values for the site occupation number operators $\hat{E}_{i,i} = \hat{n}_i$. We show the occupation numbers for these basis states for the $n = 4$ site problem (20 basis states) in Table 1, where each row is a (doublet) state. The eigenstates of the Hamiltonian are linear combination of these site basis states with coefficients determined by diagonalization of the Hamiltonian matrix. Note that it is only due to the transfer integral that the Hamiltonian matrix in the site basis is off-diagonal so that it is quite sparse. In other words, the site states diagonalize all the terms in the Hamiltonian which contain only site operators. Specifically, the part of the Hamiltonian that is diagonal is

$$H_{\text{site}} = \sum_{i=1}^{n} \alpha_i \hat{E}_{i,i} + \frac{I}{2} \sum_{i=1}^{n} \hat{E}_{i,i}(\hat{E}_{i,i} - 1) + \frac{\gamma}{2} \sum_{i,j}^{n} \hat{E}_{j,j} \hat{E}_{i,i} \qquad (2.8)$$

Equation 2.8 is, of course, the reason the site basis provides a good zero-order basis for diagonalizing the PPP Hamiltonian, eq 2.7. The two-electron operators, that are otherwise the problem, are easily handled. It is only the migration of charge from site to site that is a one-electron term that requires the numerical diagonalization of the Hamiltonian.

It is important for us to reiterate that diagonalizing the Hubbard or the PPP Hamiltonian brings about a mixing of covalent and ionic states. We emphasize that the site basis states that we used, states which are further discussed in section 3 and in Appendix A, are eigenstates of the site occupation numbers. So each basis state has a given number of electrons on a given site. The eigenstates of the Hamiltonian are linear combination of such states. The weights of the zero-order states in two different ground states are shown in Figure 1.

**TABLE 1: Site Many-Electron States for Three Electrons on Four Sites**

| | a ↑ | b ↑ | c ↑ | d ↑ | a ↓ | b ↓ | c ↓ | d ↓ |
|---|---|---|---|---|---|---|---|---|
| 1. a a<br>b | \| | \| | | | \| | | | |
| 2. a b<br>b | \| | \| | | | | \| | | |
| 3. a a<br>c | \| | | \| | | \| | | | |
| 4. a b<br>c | \| | | \| | | | \| | | |
| 5. b b<br>c | | \| | \| | | | \| | | |
| 6. a c<br>b | \| | \| | | | | | \| | |
| 7. a c<br>c | \| | | \| | | | | \| | |
| 8. b c<br>c | | \| | \| | | | | \| | |
| 9. a a<br>d | \| | | | \| | \| | | | |
| 10. a b<br>d | \| | | | \| | | \| | | |
| 11. b b<br>d | | \| | | \| | | \| | | |
| 12. a c<br>d | \| | | | \| | | | \| | |
| 13. b c<br>d | | \| | | \| | | | \| | |
| 14. c c<br>d | | | \| | \| | | | \| | |
| 15. a d<br>b | \| | \| | | | | | | \| |
| 16. a d<br>c | \| | | \| | | | | | \| |
| 17. b d<br>c | | \| | \| | | | | | \| |
| 18. a d<br>d | \| | | | \| | | | | \| |
| 19. b d<br>d | | \| | | \| | | | | \| |
| 20. c d<br>d | | | \| | \| | | | | \| |

When the site energies (the $\alpha_i$'s of eqs 2.7 or 2.8) are not equal, there is a qualitative difference in the eigenstates of the Hamiltonian when the site coupling $\beta$ is weak or strong. Charge migration is hindered when $\beta < \Delta\alpha$, where $\Delta\alpha$ is the energy difference between two adjacent sites because the wave function is localized (upper panel of Figure 1). The Hamiltonian used includes a Coulomb repulsion term, $I = 0.4$ eV, which is larger than the differences in the site energies of sites 2, 3, and 4. There are three electrons, and they settle in the ground state into the two covalent states where there is one electron on each one of these three sites, cf. Table 1. When $\beta$ is significantly larger (bottom panel of Figure 1) the wave function is delocalized on all possible doublet states. A time-dependent view of the role of $\beta/\Delta\alpha$ is also shown in Figure 3 below.

## 3. The Quantum Mechanical Charge Migration

The zero-order site basis that we use has definite occupation numbers of electrons at the different sites. An explicit example, for a three-electron four-site problem is given in Table 1, where each row is a possible state. Two particular states, rows 13 and

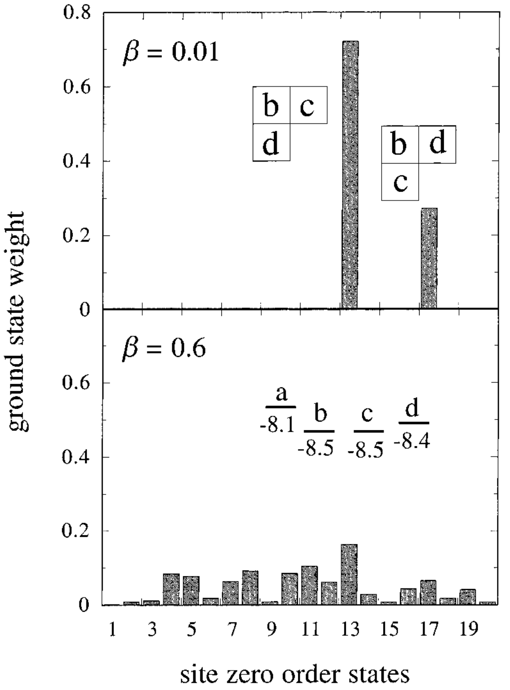

**Figure 1.** The weight of the (doublet) ground state of a three-electron four-site problem on the 20-site zero-order many-electron states. The numbering of the 20 states is that of Table 1 and the text. Upper panel: weak site−site coupling $\beta$. The ground state is localized. Lower panel: strong coupling. The sites are numbered *a* to *d*; see inset in lower panel. The label "weak" or "strong" coupling refers to $\beta$ measured with respect to the differences in the energies of the sites. Here and in Figures 2 and 4, as shown in the inset in the lower panel, $a_a = -8.1$, $a_b = -8.5$, $a_c = -8.5$, $a_d = -8.4$ all in electronvolts. The two Young tableaux shown as an insert in the upper panel are explained in Appendix A. Essentially, they mean that for weak coupling there is one electron on each one of the three sites with lower energies.

14, each one with no charge on the leftmost site, are shown in eq 3.1.

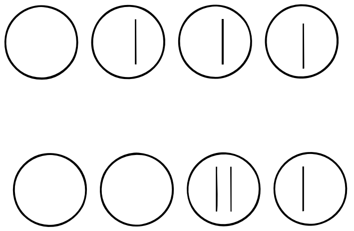

(13)

(3.1)

(14)

State 13 has every electron on a site of its own. State 14 has two electrons (of opposite spins) on the same site. Its energy can be higher because of the Coulombic repulsion, *I*, but note that the site energies need not be all the same, so states 13 and 14 can differ in energy also due to the site energies, first term in the site Hamiltonian (2.8). There are altogether eight zero-order site states (5, 8, 11, 13, 14, 17, 19, 20, cf. Table 1) with an empty leftmost site. Of these, two states (13 and 17) are covalent while the other six are ionic. These two covalent states are those occupied in the weakly coupled ground state (upper panel of Figure 1).

An initial state for charge migration into an initially empty rightmost site is a linear combination of the eight site states above. The time evolution is determined by writing the time evolution operator $U(t) \equiv \exp(-iHt/\hbar)$ as a 20 × 20 matrix in the site basis, $\mathbf{U}(t) \equiv \exp(-i\mathbf{H}t/\hbar)$ which is readily computed when the Hamiltonian matrix $\mathbf{H}$ is diagonalized. From the time-evolved wave function, expectation values of, say, the site occupancies $\langle \hat{n}_i \rangle$, $i = 1,2, ..., n$, are determined. The computational effort scales as handling $N \times N$ matrices, where $N$ is the size of the site basis.

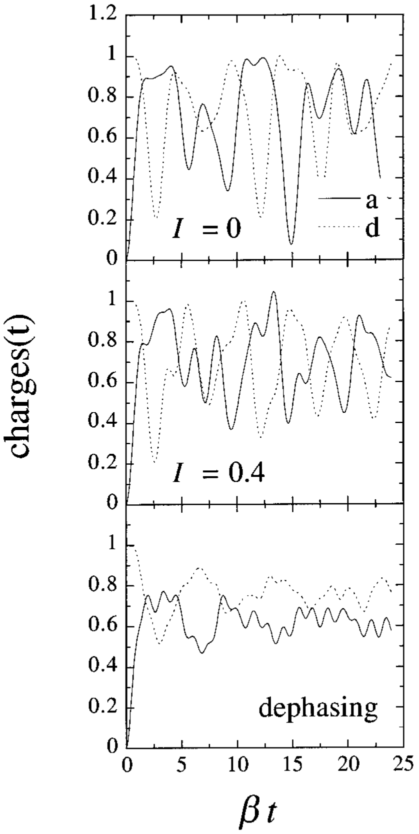

**Figure 2.** The time evolution of the charges at the two end sites, *a* and *d*, cf., Figure 1, computed quantum mechanically for an initial state with no charge at the site *a*, state 13 of the text and Table 1. Top panel: a Hückel type Hamiltonian with site−site coupling $\beta = -0.5$ eV. This is sufficient to bridge the differences in site energies (see bottom panel of Figure 1), and charge flow is quite facile. Middle panel: same as upper panel but including a repulsion between two electrons on the same site. This too is a unitary time evolution so that there is no real dephasing. There is however a defacto dephasing because with the inclusion of the Coulombic repulsion the degeneracy of covalent and ionic states is split so that there are many states with small energy spacings. Lower panel: same as middle panel but including a dephasing of the electron upon its transfer from one site to another, as in eq 2.3 with a random phase. Now, fairly quickly the charge distribution tends to equilibrate.

For $n$ sites and $N$ electrons, the number $N$ of linearly independent basis states of given total multiplicity $(2S + 1)$ is[10,32]

$$N = \frac{2S+1}{n+1}\binom{n+1}{(N-2S)/2}\binom{n+1}{(n-(N+2S)/2)} \qquad (3.2)$$

The two factors in round brackets are the binomial coefficients. For the ($n = 4$) four-site, ($N = 3$) three-electron problem that we use below as an illustration, there are $N = 20$ many-electron doublet ($S = {}^1/_2$) states. These 20 linearly independent states are shown in Table 1.

There is no problem to diagonalize the Hamiltonian for the $N = 20$ state problem. It is the exponential increase of $N$ with the number $n$ of sites that requires that we go to the classical limit, section 4. (Assuming that the number of sites, $n$, is comparable to $N$ and much larger than $S$, $N$ is of the order of $2^n$).

Figure 2 shows typical results for a problem of a charge migration in a four-site three-electron problem. The (negative) charge is initially missing from site a, the site of the lowest ionization potential (IP). In the absence of Coulomb repulsion (top panel), the charge coherently propagates up and down the chain staying mostly at the two end sites, a and d, which have the lowest IP. When Coulombic repulsion is included in the Hamiltonian, there is a more rapid spreading of the charge. There is a defacto dephasing. The Hamiltonian is purely real so that the dephasing is only apparent, being due to a sum over 20 eigenstates whose energies are different due to the removal of degeneracies by the Coulombic repulsion. One expects even more states to be mixed when three- and four-site terms are included in the Hamiltonian. We mimic this (bottom panel of Figure 2) by making the transfer amplitude $\beta$ include a scattering phase shift, eq 2.3. The first period is still coherent, but beyond it dephasing rapidly sets in.

Time in Figure 2 is scaled in units of $\beta$. This is appropriate when $\beta$ ($\beta = -0.5$ eV in Figure 2) is not small. The classical limit, discussed below, suggests for smaller $\beta$ a scaling with $\Delta\alpha$ is more suitable; see Figure 3.

## 4. The Classical Limit

The classical limit is introduced so that the computational effort scales linearly with the number of sites. The classical variables need therefore to characterize an electron, of a given spin, on a given site. We take the classical limit in a manner that ensures that the Pauli exclusion principle is satisfied. Explicitly, we associate with each site spin−orbital a fictitious spin degree of freedom. This fictitious spin is "up" when the particular site spin−orbital is occupied and is "down" when the orbital is empty. Instead of a spin, one can think of a two-level system, where one level corresponds to occupied site spin−orbital and the other to an empty site. The Pauli exclusion principle is satisfied by a level being either empty or full.

Since in the basis set there is one orbital per site, we introduce two fictitious spins per site, corresponding to the two physical spins that can be associated with each spatial orbital. Each fictitious spin gives us one classical degree of freedom.

Using the discussion in Appendix B, the correspondence between quantal operators and classical variables is as follows.

**i. Occupancies.**

$$\hat{n}_{i,\mu} \equiv a^{\dagger}_{i,\mu} a_{i,\mu} \xrightarrow{\text{classical limit}} n_{i,\mu} = (1 + \cos\theta_{i,\mu})/2 = \cos^2(\theta_{i,\mu}/2) \tag{4.1}$$

where $\hat{n}_{i,\mu}$ is the classical number of electrons of spin $\mu$ on site $i$. The origin of this correspondence is discussed in Appendix B. The introduction of the variable $\cos\theta_{i,\mu}$ as the $z$ component of the fictitious spin on site $i$ ensures that

$$0 \le n_{i,\mu} \le 1 \tag{4.2}$$

and therefore that one can introduce an angle $\theta_{i,\mu}$ such that

$$\sin\theta_{i,\mu} \equiv 2\sqrt{n_{i,\mu}}\sqrt{1 - n_{i,\mu}} \tag{4.3}$$

**ii. Creation and Annihilation Operators.**

$$\begin{aligned} a^{\dagger}_{i,\mu} &\rightarrow \frac{1}{2}\sin\theta_{i,\mu}\exp(i\phi_{i,\mu}) \\ a_{i,\mu} &\rightarrow \frac{1}{2}\sin\theta_{i,\mu}\exp(-i\phi_{i,\mu}) \end{aligned} \tag{4.4}$$

Note that, as discussed in eq B.10, $\langle a^{\dagger}\rangle\langle a\rangle \rightarrow n(1 - n)$. The angle $\phi_{i,\mu}$ is the angle conjugate to the classical action variable $n_{i,\mu}$.

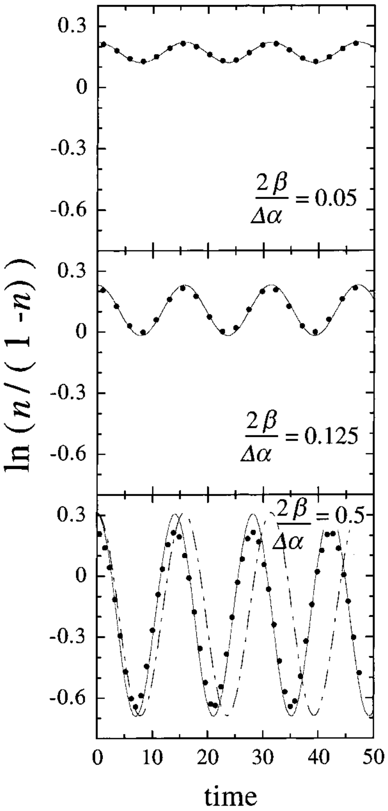

**Figure 3.** Comparing the analytical classical (curve, eq 5.4) and quantum mechanical (dots) charge migration for a two-site ($a_a = -8.1$, $a_b = -8.5$) one-electron problem. The initial occupancy of site $a$ is $n = 0.622$. When $\Delta\alpha/2\beta \gg 1$ (upper and middle panels), the analytical classical approximation is remarkably close to the exact quantum mechanical solution. When $\Delta\alpha/2\beta \le 2$ (bottom panel), the period of the classical solution is badly off (dashes). This is only to be expected because the classical solution uses an approximation, eq 4.8, which is only valid if $\Delta\alpha/2\beta > 1$. However, if we use the analytical classical result (5.4) with the ratio $\Delta\alpha/2\beta$ set to its correct value but allow $\Delta\alpha$ in the cosine term to be an adjustable parameter, the classical solution (solid line) better matches the quantum mechanical one. The fit shown here gives $\Delta\alpha = 0.43$ (instead of 0.5). The classical solution (5.4) is very sensitive to the value of $\Delta\alpha$.

The classical limit of the Hamiltonian is obtained by using the correspondence (4.1) and (4.4) in the form (2.4) of the quantal Hamiltonian. Explicitly, with the definition (2.2) of $h_{ij}$

$$\begin{aligned} H_{\text{classical}} = {} & \sum_{i}^{n}\alpha_i\sum_{\mu}^{2} n_{i,\mu} + \\ & \sum_{i,j}^{n}{}'\beta_{ij}\sum_{\mu}^{2}\sqrt{n_{i,\mu}(1 - n_{i,\mu})}\sqrt{n_{j,\mu}(1 - n_{j,\mu})}\exp(i(\phi_{i,\mu} - \phi_{j,\mu})) + \\ & \frac{1}{2} I\sum_{i} n_i(n_i - 1) + \frac{1}{2}\gamma\sum_{i,j}{}' n_i n_j \end{aligned} \tag{4.5}$$

Note that, as in quantum mechanics, classically too one can define $n_i = \sum_{\mu}^{2} n_{i,\mu}$.

The classical Hamiltonian has a form that readily lends itself to a useful interpretation of the dynamics. To see this, we begin with the one-electron part which we argue is a Hamiltonian of coupled oscillators, where the coupling is due to a, so-called,[33] 1:1 resonance. In other words, the coupling exchanges vibrational quanta from one oscillator to another. Such a transfer is physically a transfer of charge from one site to a neighboring one. The factors $\sqrt{1-n_{j,\mu}}$ ensure that a transfer is possible only to a site that is available to accommodate an electron. These factors are in fact familiar from the algebraic theory[34] of anharmonically coupled oscillators, where they represent an "anharmonicity cutoff"; that is, they disallow a transfer into a vibrational level beyond the highest level that the anharmonic well can contain.

The interpretation of the Hamiltonian follows from the classical equations of motion for action angle variables

$$\dot{n}_{i,\mu} = -\frac{\partial H}{\partial \phi_{i,\mu}}, \quad \dot{\phi}_{i,\mu} = \frac{\partial H}{\partial H n_{i,\mu}} \tag{4.6}$$

Then, the phase of the oscillator has a constant angular velocity, $\alpha_i$, with additional terms due to the coupling (which we take here to be real),

$$\dot{\phi}_{i,\mu} = \alpha_i + \beta \, ... \tag{4.7}$$

But since in general $\beta \ll \alpha$, to leading order $n_{j,\mu}$ has a constant angular velocity and the equation of motion for the phases can be integrated immediately,

$$\phi_{i,\mu}(t) = \phi_{i,\mu}(0) + \alpha_i t, \quad \beta/\Delta\alpha < 1 \text{ and } I/\Delta\alpha < 1 \tag{4.8}$$

The pairwise coupling of two oscillators is modulated by the temporal evolution of the difference in phases

$$\beta\sqrt{n_{i,\mu}(1 - n_{i,\mu})}\sqrt{n_{j,\mu}(1 - n_{j,\mu})} \exp(i(\phi_{i,\mu} - \phi_{j,\mu})) = \beta\sqrt{n_{i,\mu}(t)(1 - n_{i,\mu}(t))}\sqrt{n_{j,\mu}(t)(1 - n_{j,\mu}(t))} \exp(i((\phi_{i,\mu}(0) - \phi_{j,\mu}(0)) + (\alpha_i - \alpha_j)t)) \tag{4.9}$$

The first term of the phase in (4.9) is just a constant phase difference. It is the second term that shows the effect of a mismatch in the α's, an effect that we discussed extensively for the quantum case.[17,24] Unless the coupling $\beta$ can bridge the gap in the α's, the sites are weakly coupled. Explicitly, the prephase factor has to have a time dependence that compensates for the modulation due to the gap in the α's.

There are two other terms in $H$, the electrostatic ones. But these terms do not depend on the phase, so they do not contribute to the equation of motion of the $n$'s. Their only role is to modify the equation of motion of the phase so that (4.7) is to be replaced by

$$\dot{\phi}_{i,\mu} = \alpha_i + I n_{i,-\mu} + \frac{1}{2}\gamma \sum_j{}' \sum_{\mu}^{2} n_{j,\mu} + \beta \, ... \tag{4.10}$$

In other words, the two-electron terms make the angular frequency $n$ dependent, as for an anharmonic oscillator. The Coulomb blocking acts as a self-anharmonicity term, while the cross polarization acts as a cross anharmonicity.

## 5. Charge Migration in the Classical Limit

The classical equations of motion

$$\frac{d\phi_{i,\mu}}{dt} = \frac{\partial H}{\partial n_{i,\mu}} = \alpha_{i,\mu} + I n_{i,-\mu} + \beta\left(\frac{1 - 2n_{i,\mu}}{\sqrt{n_{i,\mu}(1 - n_{i,\mu})}}[\cos(\phi_{i,\mu} - \phi_{i+1,\mu})\sqrt{n_{i+1,\mu}(1 - n_{i+1,\mu})} + \cos(\phi_{i,\mu} - \phi_{i-1,\mu})\sqrt{n_{i-1,\mu}(1 - n_{i-1,\mu})}]\right) \tag{5.1}$$

$$\frac{dn_{i,\mu}}{dt} = -\frac{\partial H}{\partial \phi_{i,\mu}} = 2\beta[(\sqrt{n_{i,\mu}(1 - n_{i,\mu})n_{i+1,\mu}(1 - n_{i+1,\mu})} \sin(\phi_{i,\mu} - \phi_{i+1,\mu})) + (\sqrt{n_{i,\mu}(1 - n_{i,\mu})n_{i-1,\mu}(1 - n_{i-1,\mu})} \sin(\phi_{i,\mu} - \phi_{i-1,\mu}))] \tag{5.2}$$

are written here for $\gamma = 0$ so that they are not too lengthy. Even as they are they need to be integrated numerically. Checks on the integration are, as usual in classical mechanics, the back integration of the trajectory. Simpler checks are the conservation of energy, the conservation of charge, and the conservation of spin

$$H(t) = \text{const}, \quad \sum_j \sum_{\mu}^{2} n_{j,\mu}(t) = \text{const}, \quad \sum_j n_{j,\mu}(t) = \text{const for each } \mu$$

Before we show results, we discuss a simple case where an analytical solution can be obtained. This solution is both instructive and is in very good agreement with the quantal results, and so we present it in some detail.

Consider a two-site ($n = 2$) with unequal site energies. Then, with (4.9) for the coupling and using the conservation of charge and spin, one is left with only one equation of motion which we take to be the occupancy of one of the sites. We do not need a spin label because spin is conserved so that

$$\dot{n} = 2\beta n(1 - n)\sin(\Delta\alpha t) \tag{5.3}$$

The dependence of the rate of change on $n(1 - n)$ is an indication that the numerical solution will be sensitive to the magnitude of the forefactor $2\beta \sin(\Delta\alpha t)$ because this is an equation of the "logistic" type.[35]

By separation of variables and using $C$ as the constant of integration, which is determined by the initial conditions, (5.3) integrates to

$$\ln\left(\frac{n(t)}{1 - n(t)}\right) = -\frac{2\beta}{\Delta\alpha}\cos(\Delta\alpha t) + C \tag{5.4}$$

The solution is a periodic function with a periodicity determined primarily by the gap $\Delta\alpha$ in site energies, while $\beta$ determines the depth of the modulation. The larger is $\beta/\Delta\alpha$, the higher is the fraction of charge that does transfer to the other site.

Figure 3 compares eq 5.4 with the quantum mechanical results, shown as dots. When $\Delta\alpha/2\beta \gg 1$, the agreement is quite good. The quantum and classical results cannot be distinguished to graph reading accuracy. Once $2\beta/\Delta\alpha$ is larger, deviations begin to appear. These deviations are not necessarily the fault of classical mechanics but may well be due to the approximation (4.8) which we made in order to have an analytical solution. To check this, we used the analytical solution (5.4) as a fitting formula and used $\Delta\alpha$ as a free parameter. Then one obtains an excellent fit to the quantum mechanical results even when $\Delta\alpha/2\beta > 1$. The problem stems from the approximation (4.8). When $\Delta\alpha/2\beta > 1$, it is $\Delta\alpha$ that determines the period. Otherwise, the quantum mechanical solution shows that the period is the

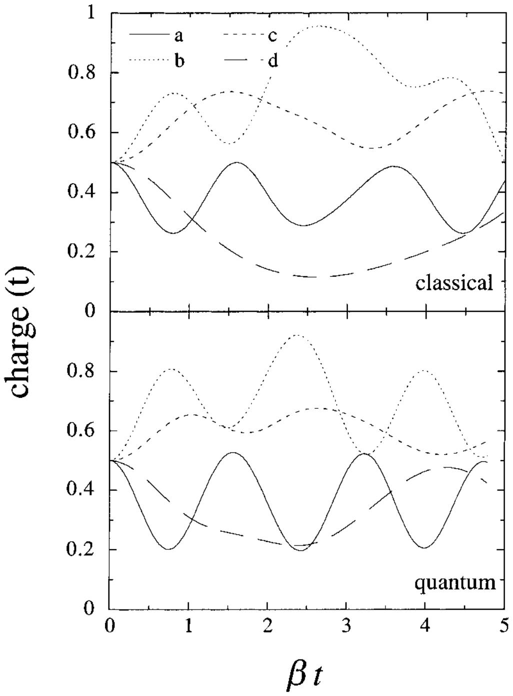

**Figure 4.** A numerical solution of the exact classical and quantum mechanical equations of motion for a (triplet) two-electron four-site problem. Site energies as in Figures 1 and 2. $\beta = -0.1$ eV. The initial state has a uniform distribution of charge. The quantum initial state is a coherent superposition of the six triplet states with equal weights. (This ensures equal charge on all four sites). The classical initial condition is $n_{i,\mathrm{up}} = 0.5$, $i = 1, ..., 4$.

spacing between the eigenstates, which in the two-state problem is

$$D = \sqrt{(\Delta\alpha)^2 + 4\beta^2} \rightarrow \begin{cases} \Delta\alpha(1 + 2\beta/\Delta\alpha + ...) \\ 2\beta(1 + \Delta\alpha/2\beta + ...) \end{cases}$$

This change in period is very evident in Figure 3.

In view of the success of the classical solution in the two-site problem, we solved the exact classical equations of motion numerically. A comparison with the quantal solution is shown for a two-electron four-site problem in Figure 4. The classical solution dephases somewhat more rapidly than the quantum mechanical solution but otherwise is able to capture the essence of the charge migration. The quantum mechanical solution shown in Figure 4 is for a real $\beta$. As we argued in section 3, this is numerically correct but physically not fully satisfactory because it fails to allow for the dephasing which does take place. So the classical solution is actually a better representation of the physical reality.

## 6. Concluding Remarks

Charge migration has been discussed with special reference to the dephasing which leads to a hopping motion of the charge. Physically, the dephasing is due to a not fully coherent transfer from one site to the next. This scattering can be due both to other electrons and to coupling to the nuclear modes. Our paper does not address the latter issue. We showed three levels of description for the role of the other electrons. (i) We included the role of electrostatic repulsion between two electrons on the same site, the Hubbard correction, and on other sites, the Pariser−Parr−Pople correction. This effect was solved for exactly using a unitary group many-electron basis (Appendix A) and was shown to lead to some dephasing, Figure 2. (ii) We included the role of electrostatic repulsion as in (i) and, in addition, elastic scattering of the transferred electron, eq 2.3. Finally, (iii) we introduced a classical limit (Appendix B) of the dynamics. The classical approximation was remarkably realistic, and we intend to use it for bigger systems for which the exact quantum mechanics is computationally intractable.

**Acknowledgment.** This work was supported by the Volkswagen Foundation and used computational facilities of SFB 377. We thank the Commissariat Général aux Relations Internationales de la Communauté Française de Belgique (CGRI) and the Israeli Government for a fellowship to F.R.

## Appendix A: The Construction of the Many-Electron Basis

Equation 3.2 specifies that there are $N = 20$ doublet ($S = {}^1/_2$) states corresponding to a ($n = 4$) four-site, ($N = 3$) three-electron system. These states are shown schematically in Table 1. Each row is a site state. The columns are the four sites and spin labels such that each site carries two spin−orbitals, but what is spin up or down is arbitrary. Only the total spin matters. The bars show the occupancy.

There are several ways to classify and enumerate the spin-adapted many-electron states. These are reviewed in detail elsewhere.[32] In this paper, we use the Paldus states[10] to generate the matrix elements of the Hamiltonian in the many-electron site basis and we show in Table 1 the Young tableaux[36] which correspond to these Paldus states.

**i. Paldus States.** All the orthonormal spin-adapted $N$ electron states can be generated from the highest weight vector, in Paldus [10]notation ($a$, $b$, $c$) where $a$, $b$ and $c$ are given by

$$a + b + c = n, \quad 2a + b = N, \quad b = 2S \tag{A.1}$$

For Table 1, $(a, b, c) \equiv (1, 1, 2)$. To identify the highest row of the Paldus tableau, we designate ($a$, $b$, $c$) above as $(a_n, b_n, c_n)$.[10,32] The highest row of the tableau is then the highest weight vector.

The many-electron states are represented as three-column Paldus tableaux, built of $n$ rows $(a_i, b_i, c_i)$, $i = 1, ..., n$. The entries of the different rows are recursively obtained from the highest weight vector $(a_n, b_n, c_n)$. These $n \times 3$ matrices have only nonnegative entries and for each row, $a_i + b_i + c_i = i$, so that the Paldus tableau of $(n - i)$ rows belongs to $U(n - i)$ and corresponds to a system with $(n - i)$ orbitals and $n_{n-i} = (a_{n-i} - a_{n-i-1}) + (1 - (c_{n-i} - c_{n-i-1}))$, $(a_0 = c_0 = 1)$ electrons. These $n_{n-i}$ electrons are coupled to the electrons of the intermediate level $(n - i - 1)$ of intermediate spin $\mathrm{S}_{n-i-1}$ in such a way that the spin $S_{n-i} = ({}^1/_2)\mathrm{b}_{n-i}$ characteristic of the $(n - i)$th row is obtained. All the $N$ Paldus tableaux differ by at least a row and have the same $n$th row, which is the highest weight vector $(a_n, b_n, c_n)$.

We show below the Paldus tableaux corresponding to the site many-electron states 13 and 14,

$$\begin{array}{c} \mathrm{d} \\ \mathrm{c} \\ \mathrm{b} \\ \mathrm{a} \end{array} \underset{(13)}{\begin{bmatrix} 1 & 1 & 2 \\ 1 & 0 & 2 \\ 0 & 1 & 1 \\ 0 & 0 & 1 \end{bmatrix}} \qquad \underset{(14)}{\begin{bmatrix} 1 & 1 & 2 \\ 1 & 0 & 2 \\ 0 & 0 & 2 \\ 0 & 0 & 1 \end{bmatrix}} \tag{A.2}$$

where $a$, $b$, $c$, and $d$ are the labels of the $n = 4$ sites. The orbital occupancies of these states are also shown in eq 3.1 of the text.

**ii. Young Tableaux.** To satisfy the Pauli principle, a site can be occupied by at most two electrons, which means that the $N$ electron states are represented by $N$ boxes arranged in two columns at most. The total spin is given by the length difference between the two columns. For $N = 3$ doublet states, one column has a length of two boxes and the other one consists of a single box. One column corresponds to electrons of a given spin and the other column has electrons of opposite spin. To outline correspondence between the Paldus states and the Young tableaux, one needs to rewrite the Paldus states in terms of two column, $n$ row tableaux, known as the $\Delta AC$ tableaux[32] where the entries, $\Delta a_k$, of the first column are defined as

$$\Delta a_k = a_k - a_{k-1} \tag{A.3}$$

while the entries, $\overline{\Delta c_k}$, of the second column are given by

$$\overline{\Delta c_k} = 1 - \Delta c_k \quad \text{with} \quad \Delta c_k = c_k - c_{k-1} \tag{A.4}$$

Within this notation, the occupation number of site $k$ is given by

$$n_k = \Delta a_k + \overline{\Delta c_k} \tag{A.5}$$

It is possible to show [32] that the entries $\Delta a_k$ and $\overline{\Delta c_k}$ completely specify the many-electron states so that the three columns $n$ row shown in eq A.2 are completely equivalent to the following two-column $n$ row tableaux:

$$\begin{array}{c} \mathrm{d} \\ \mathrm{c} \\ \mathrm{b} \\ \mathrm{a} \\ \phantom{(13)} \end{array} \begin{array}{c} \begin{bmatrix} 0 & 1 \\ 1 & 0 \\ 0 & 1 \\ 0 & 0 \end{bmatrix} \\ (13) \end{array} \qquad \begin{array}{c} \begin{bmatrix} 0 & 1 \\ 1 & 1 \\ 0 & 0 \\ 0 & 0 \end{bmatrix} \\ (14) \end{array} \tag{A.6}$$

The Young tableau shown in Table 1 are thus obtained by inserting in the boxes of the first column the row labels for which $\overline{\Delta c_k} = 1$ and in the boxes of the second column, the row labels for which $\Delta a_k = 1$ gives for the two states above:

$$\begin{array}{c} \begin{array}{|c|c|} \hline \mathrm{b} & \mathrm{c} \\ \hline \mathrm{d} & \\ \hline \end{array} \\ (13) \end{array} \qquad \begin{array}{c} \begin{array}{|c|c|} \hline \mathrm{c} & \mathrm{c} \\ \hline \mathrm{d} & \\ \hline \end{array} \\ (14) \end{array} \tag{A.7}$$

**iii. Matrix Elements of the Hamiltonian in the Paldus States.** The analytical expressions of the matrix elements of the Hamiltonian in the spin-adapted site many-electron state basis set are given in terms in the Paldus states in refs 10, 17, and 32. They are obtained using the commutation relations of the $E_{i,j}$ generators of the group $U(n)$,

$$[E_{ij}, E_{kl}] = E_{il}\delta_{jk} - E_{kj}\delta_{il} \tag{A.8}$$

## Appendix B: The Classical Limit

When the number, $n$, of sites is not small, the basis size increases exponentially, cf., eq 3.2. It is then no longer practical to diagonalize the Hamiltonian as a symmetric matrix, particularly so when the array of sites is two (or more) dimensional and there are more than two near neighbors of a given site. It is still possible to defacto diagonalize the Hamiltonian using a filter diagonalization[37,38] or similar methods. Here, however, we examine an alternative route, namely, taking a classical limit and solving the classical equations of motion.

It is well-known and goes back to Dirac[39] that quantum mechanics can be transcribed as a problem in classical mechanics if one introduces a classical degree of freedom for every accessible basis *state* of the quantum mechanical problem. See, for example, ref 40 for a practical realization. This, however, will not allow a simple scaling of the computational effort with the size of the system. Rather, we need a scheme that assigns one classical degree of freedom per *particle*. Moreover we would like to be consistent with the Pauli principle; that is, we want to ensure that there is not more than one electron of a given spin on a given site. If it were not for this restriction then one knows quite well what to do: an annihilation (or creation) operator of a particle in a given site is represented by the polar operator form[41]

$$\begin{aligned} a^\dagger &\rightarrow \sqrt{\hat{n}}\,\exp(-i\hat{\phi}) \\ a &\rightarrow \exp(i\hat{\phi})\sqrt{\hat{n}} \end{aligned} \tag{B.1}$$

The operators carry the label of the site which, in the appendix, we do not explicitly display. Then, if $\hat{n}$ and $\hat{\phi}$ are regarded as conjugate variables,

$$[\hat{n}, \hat{\phi}] = i \tag{B.2}$$

The definition (B.2) is equivalent to the boson commutation relation $[a,a^\dagger] = 1$. It is now possible to take the classical limit by the Dirac prescription of replacing the commutator of the operators by the Poisson bracket of the classical variables,

$$i = [\hat{n},\hat{\phi}] \rightarrow i\{\hat{n},\hat{\phi}\} \tag{B.3}$$

This shows that in the classical limit $n$ and $\phi$ are action-angle variables. There are problems with the interpretation of $\hat{n}$ and $\hat{\phi}$ as Hermitian operators,[42,43] but this is not our primary concern. From our point of view the issue is that the correspondence (B.1) between creation and annihilation operators and action-angle variables is valid for operators which satisfy *boson* statistics. The creation and annihilation operators, used to define the quantum mechanical Hamiltonian (2.4), obey *fermion* statistics

$$[a,a^\dagger]_+ \equiv aa^\dagger + a^\dagger a = 1 \tag{B.4}$$

This can be used to show that the corresponding number operator $E, E \equiv a^\dagger a$, has only two eigenvalues, 0 and 1, a result that we know as the Pauli exclusion principle. Our problem is to obtain a classical limit for such fermion operators. The prescription that we found in the literature [44] is to use "anticommuting numbers" sometimes known as Grassmann variables. Instead we proceeded as follows.

The Pauli spin matrices, defined as usual,

$$\sigma_\pm \equiv \frac{1}{2}(\sigma_1 \pm i\sigma_2)\text{or } \sigma_+ = \begin{pmatrix} 0 & 1 \\ 0 & 0 \end{pmatrix},\ \sigma_- = \begin{bmatrix} 0 & 0 \\ 1 & 0 \end{bmatrix} \tag{B.5}$$

satisfy the anticommutation relation $[\sigma_+,\sigma_-]_+ = 1$ identical to that of the fermion creation and annihilation operators. The role of the number operator is provided using the third Pauli matrix,

$$\sigma_3 = \begin{pmatrix} 1 & 0 \\ 0 & -1 \end{pmatrix},\quad \frac{1}{2}(1 + \sigma_3) = \sigma_+\sigma_- \tag{B.6}$$

We go to the classical limit by taking the (spin) coherent states expectation values. The coherent states convenient for our purpose are where the spin points out in the direction of the solid angle $\Omega$[45]and the states are normalized,

$$\langle\Omega|\hat{S}|\Omega\rangle = \frac{1}{2}\mathbf{n} \tag{B.7}$$

**n** is the unit vector in the direction of $\Omega$, and we took the spin of the particle to be one-half. For these states,[45] and using carats to designate operators,

$$\begin{aligned}\langle\Omega|\hat{S}_+|\Omega\rangle &= \frac{1}{2}\sin\theta\exp(i\phi)\\ \langle\Omega|\hat{S}_-|\Omega\rangle &= \frac{1}{2}\sin\theta\exp(-i\phi)\\ \langle\Omega|\hat{S}_+\hat{S}_-|\Omega\rangle &= \left\langle\Omega\left|\frac{1}{2}(1+\hat{S}_z)\right|\Omega\right\rangle = \frac{1}{2}(1+\cos\theta)\end{aligned} \tag{B.8}$$

Using the correspondence

$$a^\dagger a \rightarrow \cos^2\left(\frac{\theta}{2}\right) \equiv n \tag{B.9}$$

so that the classical number variable satisfies the exclusion principle, $0 \le n \le 1$, we obtain the classical limit for the fermion creation and annihilation operators

$$\begin{aligned} a^\dagger &\rightarrow \frac{1}{2}\sin\theta\exp(i\phi) = \sqrt{n(1-n)}\exp(i\phi)\\ a &\rightarrow \frac{1}{2}\sin\theta\exp(-i\phi) = \sqrt{n(1-n)}\exp(-i\phi)\end{aligned} \tag{B.10}$$

Note that in terms of (coherent states) expectation values $n \leftarrow \langle a^\dagger a\rangle \neq \langle a^\dagger\rangle\langle a\rangle \rightarrow n(1-n)$ so that there is no inconsistency between (B.9) and (B.10). Indeed, since $n^2 \le n$, this is as it should be.

**The Boltzmann Limit.** We do not use the limit where the effects of the Pauli statistics are negligible, but for completeness we derive it. Say the spin $S$ is high. For an arbitrary spin, (B.8) is replaced by

$$\begin{aligned}\langle\Omega|\hat{S}_+|\Omega\rangle &= S\sin\theta\exp(i\phi)\\ \langle\Omega|\hat{S}_-|\Omega\rangle &= S\sin\theta\exp(-i\phi)\\ \langle\Omega|\hat{S}_+\hat{S}_-|\Omega\rangle &= \langle\Omega|(1+\hat{S}_z)|\Omega\rangle = S(1+\cos\theta)\end{aligned} \tag{B.11}$$

Then, instead of (B.10), we find

$$\begin{aligned} a^\dagger &\rightarrow \frac{1}{2}\sin\theta\exp(i\phi) = \sqrt{n(2S-n)}\exp(i\phi)\\ a &\rightarrow \frac{1}{2}\sin\theta\exp(-i\phi) = \sqrt{n(2S-n)}\exp(-i\phi)\end{aligned} \tag{B.12}$$

In the limit $S \rightarrow \infty$, we recover the classical limit for the boson operators. The "correction" factor $\sqrt{n(2S-n)}$ is familiar from the algebraic theory of anharmonic molecules, where $n$ is the vibrational quantum number and $2S$ is the number of bound states. Here too, this factor serves to limit the range of $n$. The trick of taking the limit of high $S$ is the, so-called contraction that is used to get the harmonic limit.[46,47] For completeness, we also note that there is more than one way in which one can take the high $S$ limit. A simple illustrative case is a quantal Morse oscillator. When taking its classical limit we want the anharmonicity to remain finite. So the $S \rightarrow \infty$ limit must be taken with $\hbar \rightarrow 0$ so as to keep the anharmonicity finite. (see note 7.5 of ref 48). On the other hand, if we keep $\hbar$ finite but take the high $S$ limit, we get the harmonic quantal oscillator.

## Summary

We use the correspondence

$$\begin{aligned} a^\dagger &\rightarrow \sqrt{n(1-n)}\exp(i\phi)\\ a &\rightarrow \sqrt{n(1-n)}\exp(-i\phi)\\ a^\dagger a &\rightarrow n\end{aligned} \tag{B.13}$$

where $n$ and the phase $\phi$ carry both a site and a spin label and $n_{i,\mu}$, $0 \le n_{i,\mu} \le 1$, is the fraction of electrons on the spin-orbital of spin $\mu$ on the $i$th site. The classical limit of the Hamiltonian is obtained by using (B.13) in the quantum mechanical Hamiltonian.

**Note added in proof:** Prof. Witt. Miller called our attention to a similar development by Miller and White (*J. Chem. Phys.* **1986**, *84*, 5059).

## References and Notes

(1) Hoffmann, R. *Solids and Surfaces: A Chemist's View of Bonding in Extended Structures*; VCH: New York, 1988.

(2) Hehre, W. J.; Radom, L.; Schleyer, P. v. R.; Pople, J. A. *Ab Initio Molecular Theory*; Wiley: New York, 1986.

(3) Coulson, C. A.; Fischer, I. *Philos. Mag.* **1949**, *40*, 386.

(4) Bobrowicz, F. W.; Goddard, W. A. In *Methods of Electronic Structure Theory;* Schaefer, H. F., Ed.; Plenum: New York, 1967.

(5) Goddard, W. A. *Phys. Rev.* **1967**, *157*, 81.

(6) Goddard, W. A. *J. Am. Chem. Soc.* **1972**, *94*, 793.

(7) Hubbard, J. *Proc. R. Soc.* **1963**, *276*, 238.

(8) Parr, R. G. *Quantum Theory of Molecular Electronic Structure*; Benjamin: New York, 1963.

(9) Schatz, G. C.; Ratner, M. A. *Quantum Mechanics in Chemistry*; Prentice Hall: New York, 1993.

(10) Paldus, J. *J. Chem. Phys.* **1974**, *61*, 5321.

(11) Matsen, F. A. *Int. J. Quantum Chem. Symp.* **1974**, *8*, 379.

(12) Shavitt, I. In *The Unitary Group for the Evaluation of Electronic Energy Matrix Elements*; Hinze, J., Ed.; Springer-Verlag: Berlin, 1981.

(13) Pauncz, R. *Spin Eigenfunctions: Construction and Use*; Plenum: New York, 1979.

(14) *The Unitary Group for the Evaluation of Electronic Energy Matrix Elements*; Lecture Notes in Chemistry; Hinze, J., Ed.; Springer: Berlin, 1981.

(15) Ziman, J. M. *Principles of the Theory of Solids*; Cambridge Univeristy Press: Cambridge, 1965.

(16) Madelung, O. *Introduction to Solid-State Theory*; Springer: Berlin, 1996.

(17) Remacle, F.; Levine, R. D. *J. Chem. Phys.* **1999**, 5089.

(18) Kosloff, R.; Ratner, M. A. *Isr. J. Chem.* **1990**, *30*, 45.

(19) Markovich, G.; Collier, C. P.; Henrichs, S. E.; Remacle, F.; Levine, R. D.; Heath, J. R. *Acc. Chem. Res.* **1999**, *32*, 415.

(20) Remacle, F.; Collier, C. P.; Heath, J. R.; Levine, R. D. *Chem. Phys. Lett.* **1998**, *291*, 453.

(21) Born, M. *The Mechanics of the Atom*; G. Bell and Sons: London, 1967.

(22) Goldstein, H. *Classical Mechanics*; Addison-Wesley: Reading, 1980.

(23) Weinkauf, R.; Schlag, E. W.; Martinez, T. J.; Levine, R. D. *J. Phys. Chem. A* **1997**, *101*, 7702.

(24) Remacle, F.; Levine, R. D.; Ratner, M. A. *Chem. Phys. Lett.* **1998**, *285*, 25.

(25) Remacle, F.; Levine, R. D.; Schlag, E. W.; Weinkauf, R. *J. Phys. Chem. A* **1999**, *103*, 10149.

(26) Weinkauf, R.; Schanen, P.; Metsala, A.; Schlag, E. W.; Buergle, M.; Kessler, H. *J. Phys. Chem.* **1996**, *100*, 18567.

(27) *Electron transfer: From Isolated Molecules to Biomolecules*; Jortner, J., Bixon, M., Eds.; Advances in Chemical Physics; Wiley: New York, 1999.

(28) Newton, M. D. *Chem. Rev.* **1991**, *91*, 767.

(29) *Molecular Electronics*; Jortner, J., Ratner, M., Eds.; Blackwell Science: Cambridge, MA, 1997.

(30) Linderberg, J.; Öhn, Y. *Propagators in Quantum Chemistry*; Academic Press: New York, 1973.

(31) Calais, J. L.; Deumens, E.; Öhn, Y. *J. Chem. Phys.* **1994**, *101*, 3989.

(32) Paldus, J. In *The Unitary Group for the Evaluation of Electronic Energy Matrix Elements;* Hinze, J., Ed.; Lecture Notes in Chemistry 22; Springer: Berlin, 1981.

(33) Rice, S. A. *Adv. Chem. Phys.* **1981**, *47*, 117.

(34) Benjamin, I.; Levine, R. D.; Kinsey, J. L. *J. Phys. Chem.* **1983**, *87*, 727.

(35) Reichl, L. E. *The Transition to Chaos in Conservative Classical Systems: Quantum Manifestation*; Springer-Verlag: Berlin, 1992.

(36) Moshinsky, M. In *Many Body Problems and Other Selected Topics in Theoretical Physics*; Moshinsky, M., Brody, T. A., Jacob, G., Ed.; Gordon and Breach: New York, 1966.

(37) Wall, M. R.; Neuhauser, D. *J, Chem. Phys.* **1995**, *102*, 8011.

(38) Mandelshtam, V. A.; Grozdanov, T. P.; Taylor, H. S. *J. Chem. Phys.* **1995**, *103*, 10074.

(39) Dirac, P. A. M. *Proc. R. Soc. A* **1927**, *114*, 243.

(40) Meyer, H.-D.; Miller, W. H. *J. Chem. Phys.* **1979**, *71*, 2156.

(41) Heitler, W. *Quantum Theory of Radiation*; Oxford University Press: Oxford, 1954.

(42) Carruthers, P.; Nieto, N. M. *Phys. Rev. Lett.* **1965**, *14*, 387.

(43) Levine, R. D. *J. Chem. Phys.* **1966**, *44*, 2035.

(44) Klauder, J. R.; Skagerstam, B. S. *Coherent States: Applications in Physics and Mathematical Physics*; World Scientific: Singapore, 1985.

(45) Radcliffe, J. M. *J. Phys. A* **1971**, *4*, 313.

(46) Holstein, T.; Primakoff, H. *Phys. Rev.* **1940**, *58*, 1098.

(47) Levine, R. D. In *Intramolecular Dynamics*; Jortner, J., Pullman, B., Ed.; Reidel: Dordrecht, 1982.

(48) Iachello, F.; Levine, R. D. *Algebraic Theory of Molecules*; Oxford University Press: New York, 1995.